Atmospheric Research 204 (2018) 94–101

Contents lists available at ScienceDirect

Atmospheric Research

journal homepage: www.elsevier.com/locate/atmosres

The role of natural mineral particles collected at one site in Patagonia as immersion freezing ice nuclei

María Laura López[a,*], Laura Borgnino[b], Eldo E. Ávila[a]

[a] IFEG-CONCIET-FaMAF, Universidad Nacional de Córdoba, Córdoba, Argentina
[b] CICTERRA-CONICET, Universidad Nacional de Córdoba, Córdoba, Argentina

ARTICLE INFO

Keywords:
Ice nuclei particles
Immersion freezing
Patagonia
Soil particles
Feldspars

ABSTRACT

This work studies the role of mineral particles collected in the region of Patagonia (Neuquén, Argentina) as ice nuclei particles (INPs) by immersion freezing mode. The particle immersion-freezing ability was analyzed under laboratory conditions by using an established drop-freezing technique. Mineralogical composition was characterized by using X-ray diffraction and electron micro probe analysis. Dynamic light scattering was used to determine the grain size distribution of particles, while the N_2 adsorption and methylene blue adsorption methods were applied to determine their specific surface area. Water droplets of different volumes containing different concentrations of particles were cooled until droplets were frozen. For all the analyzed drop volumes, an increase in the freezing temperature of the drops was observed with increasing dust concentration. In the same way, the freezing temperature increased when the drop volume was increased at constant dust concentration. Both behaviors were linked to the availability of active sites in the particles. A plateau in the freezing temperature was observed at high suspension concentration for all the drop volumes. This plateau was related to the aggregation of the particles when the suspension concentration was increased and to the consequent decrease in the number of active sites. The active sites per unit of surface area were calculated and reported. For the studied range of temperature, results are in agreement with those reported for different sites and particles. From the chemical and morphological analysis of the particle components and the results obtained from the literature, it was concluded that even though montmorillonite was the main mineral in the collected sample, the accessory minerals deserve to be analyzed in detail in order to know if they could be responsible for the ability of the collected soil particles to act as INPs. Considering that the region of Patagonia has been identified as an important source of natural mineral particles in the atmosphere, it is important to analyze the ability of these particles to act as INP. As far as we know, this is the first study carrying out this investigation.

1. Introduction

Heterogeneous nucleation is the main process forming ice in the atmosphere, which involves the foreign surfaces of insoluble particles called ice nuclei particles (INP). The chemical and physical characteristics of the aerosol particles acting as INPs are a topic of intense research (e.g. Santachiara et al., 2010; Yang et al., 2014). It has been shown that primary biological particles, mineral dust, metallic particles, soot, and volcanic ash, act as INPs (Fröhlich-Nowoisky et al., 2016; Hazra et al., 2016; Popovicheva et al., 2008; Von Blohn et al., 2005).

There are four modes involving heterogeneous nucleation: deposition nucleation, condensation freezing, contact freezing, and immersion freezing. Deposition nucleation occurs when ice is deposited on the INPs from the vapor phase. For this reason, the environment can be subsaturated with respect to liquid water, but supersaturated with respect to ice. Condensation freezing occurs at temperatures below 0 °C when cloud condensation nuclei act as INPs. During contact freezing, the ice is formed by the collision of interstitial aerosols with cloud droplets. Lastly, immersion freezing occurs when INPs are immersed in aqueous droplets at temperatures below 0 °C (Vali, 1985).

The immersion freezing mechanism is involved in the formation of ice crystals in cirrus and mixed-phase clouds (e.g. Hoose and Möhler, 2012). A review of particles immersed in supercooled droplets acting as INPs has been compiled by Murray et al. (2012). Mineral dust particles play a dominant role in ice formation by immersion freezing (Hoose et al., 2010). At the same time, natural mineral dust particles make the largest mass contribution to aerosol in the atmosphere (e.g. Satheesh and Moorthy, 2005). For this reason, recent works have been focused on understanding the role of mineral particles as INPs by immersion freezing. A recent comparison of the laboratory techniques used to

* Corresponding author.
E-mail address: laulopez@famaf.unc.edu.ar (M.L. López).

https://doi.org/10.1016/j.atmosres.2018.01.013
Received 7 September 2017; Received in revised form 10 January 2018; Accepted 19 January 2018

examine immersion freezing activity was made by Hiranuma et al. (2015). This laboratory studies use commercial particles as surrogates for atmospheric mineral dust particles (e.g. Nagare et al., 2016; Wex et al., 2014) or natural mineral particles. One of the most recent works showing the efficiency of these natural mineral particles in the immersion freezing mode is presented by Kaufmann et al. (2016).

Considering that clay minerals (mainly kaolinite, montmorillonite, or illite) are the main components of mineral dust particles and the most common minerals transported in the atmosphere, they have been intensively studied as INPs by immersion freezing mode (Murray et al., 2012; Boose et al., 2016). However, recently Atkinson et al. (2013) have shown that the feldspar component is more efficient at nucleating ice than other minerals present in higher proportion in desert dusts. Moreover, Harrison et al. (2016) and Kaufmann et al. (2016) showed that the role of feldspar particles promoting the immersion freezing is related to the polymorphic forms of the structures of the feldspars. Thus, the impact of mineral dust aerosols on ice formation depends strongly on their mineralogy, which is largely variable both geographically and spatially (Formenti et al., 2014).

The arid regions around the world have been identified as the most important sources of natural mineral particles in the atmosphere (Prospero et al., 2002; Ginoux et al., 2012). The main arid regions are the global dust belt from the Sahara to the Taklamakan in China, the deserts located in the USA and Mexico, Australia, Botswana, Namibia, Bolivia, and Patagonia in western Argentina (e.g. Formenti et al., 2011). The last five regions are the main sources located in the Southern Hemisphere. Over the last 50 years, the role of mineral dusts from Sahara and arid regions in Asia has been related to heterogeneous nucleation (e.g. Isono et al., 1959; Belosi et al., 2017).

Regarding the Southern Hemisphere, even though some recent works have analyzed the heterogeneous nucleation on natural particles collected in Botswana, Namibia, Bolivia, and Australia (Kaufmann et al., 2016; Boose et al., 2016), there is still a lack of measurements in this area. Indeed, studies of natural dust particles as INPs from Patagonia have never been reported. This area is worth analyzing because Patagonia is the most important source of dust in South America (Prospero et al., 2002) and because the particles can even reach Antarctica (Gassó et al., 2010), where ice formation is important since clouds are prevalently mixed or cold (e.g. Belosi et al., 2014).

In this context, the aim of the present study was to characterize the ability of soil mineral particles collected in the region of Patagonia to act as ice nuclei particles by immersion freezing mode. As far as we know, this is the first work studying the role of Patagonian soil particles as INP.

2. Materials and methods

2.1. Mineral dust particles

Patagonia is located between latitudes 38° and 52°, stretching over about 700,000 km^2 and covers practically the whole of south Argentina. The climate is controlled by the dynamics of westerly winds, which blow from the South Pacific Ocean. Since most of their moisture is discharged on the Andes, they continue as dry winds to the east. As a consequence, rainfall in the region is low, with a mean annual precipitation of 100–180 mm (National Weather Office). The monthly mean velocity of the western winds is 30 km h^{-1}. The maxima are recorded during October (spring time), when wind velocity can be over 100 km h^{-1}. Winds blowing from the east (Atlantic Ocean) are calmer, except during some storms concentrated mainly in July. The dust storms are very frequent in Patagonia and they are mainly related to the western winds from the Andes (Ramsperger et al., 1998a, 1998b).

The semi-arid plateau of northern Patagonia is almost treeless, with vegetation covering around 30%. The combination of sparse vegetation, high wind velocity and low water content in soil becomes an important soil erosion factor and the transport of aerosol particles in the atmosphere (Tegen and Fung, 1994). In fact, Patagonia and Australia constitute the predominant sources of dust delivered on the surface of the South Atlantic Ocean (e.g. Johnson et al., 2010; Gaiero et al., 2003). Prospero et al. (2002) showed that the main source of dust in Patagonia is located between 38° S and 48° S. Within this region, they identified a particular source in the province of Neuquén, on the flanks of the Andes, and in western Río Negro. In this area, which is part of the Neuquén Basin, there are many bentonite deposits (e.g. Domínguez et al., 2001) which extends to the extra-Andean Region at the provinces of Río Negro, La Pampa and Neuquén (around 120,000 km^2). For the present work, this area was selected to collect natural mineral samples. Even bentonites are present along all the Patagonia region (e.g. McCartney, 1934), they were formed in different geological periods. In the present work, sample was collected in the province of Neuquén, in northern Patagonia. The area of collection is in the surroundings of a hill called Cerro Bandera located at latitude 38.75° S and longitude 70.33° W, and 1103 m a.s.l., where deposits of bentonite occur with 2 to 15 m in thickness (Impiccini and Vallés, 2002). Thus, the collected sample would correspond to a bentonite from the Tertiary period (Impiccini and Vallés, 2002; Domínguez et al., 2001). Then, we estimate the collected sample is representative of an approximate area of 6000 km^2. The collection site was selected because it is located in an area identified as the main source of dust in Patagonia region (Prospero et al., 2002). This choice was also based in the results from Gaiero et al. (2004). From the analysis of the rare earth element (REE) signature of dust, topsoil and riverine sediments in Patagonia, they showed that eolian dust exhibits REE compositions similar to Patagonian topsoils. This is why Patagonian topsoils has been identified as important contributors to the eolian dust, which is delivered to the South Atlantic Ocean (Gaiero et al., 2003, 2004).

The sample was collected from a sediment profile, in the bottom section located at 1 m from the surface in order to avoid the organic matter contamination. XRD and EDX analysis were used to verify the sample was only composed by mineral matter. Fig. 1 shows a map of the study area and the location of the sampling site. In order to characterize the collected particles, the X-ray diffraction and electron micro probe analysis techniques were used to analyze the chemical composition of the particles. The specific surface area of the particles was measured by the N_2 adsorption and methylene blue adsorption methods. The grain size distribution of the collected particles was measured by using the dynamic light scattering method.

2.1.1. X-ray diffraction

Powder X-ray diffraction (XRD) was used to determine the main minerals present in the sample. XRD patterns were recorded on a Philips X'Pert PRO X-ray diffractometer, using CuK radiation (30 kV-15 mA). Data were obtained in the 2θ range of 4 to 70° (step size: 0.01; 6 seg step^{-1}). The reflection assignments were carried out using the Panalytical X'Pert High Score software. Fig. 2 shows the XRD spectrum of the analyzed sample. The presence of the 001 reflection at 7.01 2θ corresponding to a basal spacing d_{001} of 12.6 Å is typical for a Na exchanged montmorillonite (Borgnino et al., 2009). Other mineral phases (quartz and feldspar) are also present as accessory minerals, which lead us to classify the collected sample as a bentonite in agreement with previous mineralogical studies (Impiccini and Vallés, 2002).

2.1.2. Electron micro probe analysis

The chemical composition of the sample was determined by electron micro probe analysis (EMPA). A JEOL JXA 8230 microprobe at the LAMARX laboratory of the National University of Córdoba, operating in wavelength-dispersive mode (WDS) was used. Before analysis, samples were gently disaggregated with a pestle and mortar and then mixed with Epofix resin and hardener. After that, the samples were placed in a pressure vessel for 12 h, then backfilled with araldite resin and dried in an oven (50 °C, ≥ 4 h). To perform the measures, the samples were polished and subsequently carbon coated before being measured. The

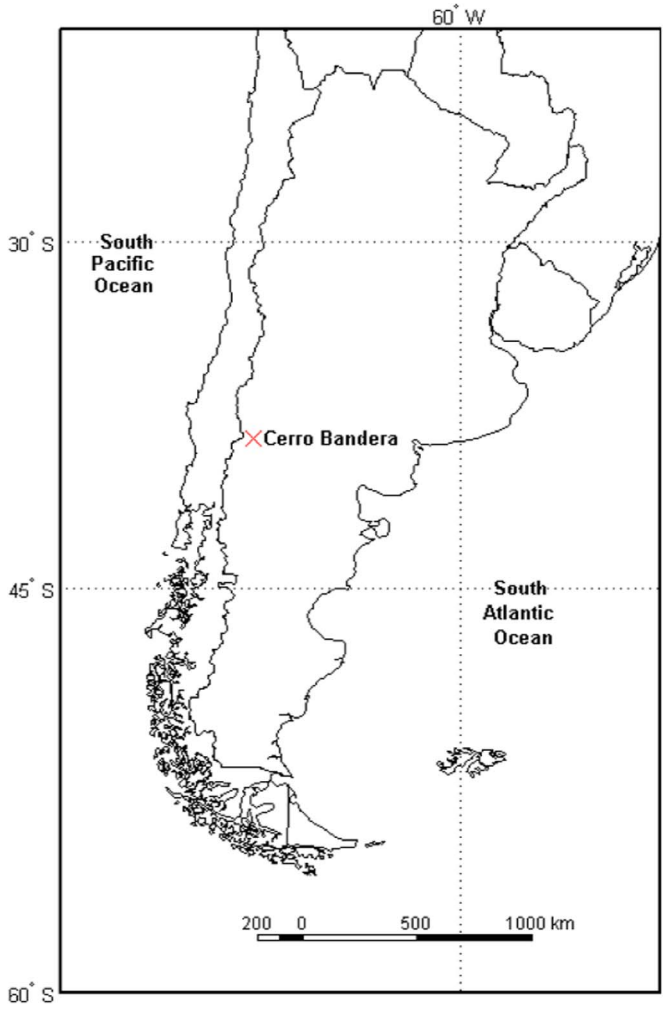

Fig. 1. Location of the sampling site.

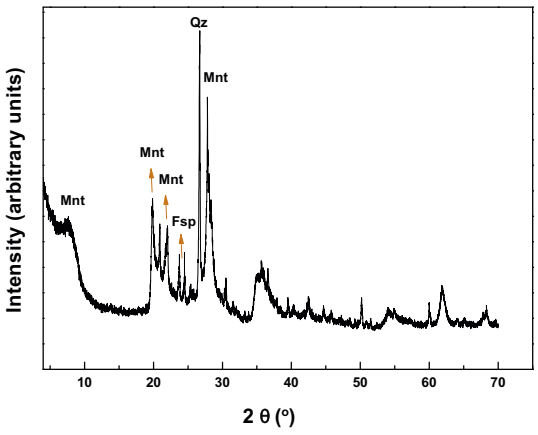

Fig. 2. XRD patterns of the studied sample. Reflections assignments are as follows: Mnt, montmorillonite; Qz, quartz; Fsp, feldspar.

analytical conditions were as follows: 15 kV acceleration potential, 7 nA beam current and a beam diameter of 8 μm. The counting times for Na, K, and Si were firstly measured within 5 s (one on each spectrometer) in order to minimize varying count rates produced by alkali migration and Si "grow-in". The counting times for other elements were 10 s (Al, Ca, Mg, Fe, Mn, Cl) and 15 s (Ti and P), with half times at each background position. The standards were: albite (Na), anorthoclase (Al, Si), orthoclase (K), ilmenite (Ti), forsterite (Mg), fayalite (Fe), wollastonite (Ca),

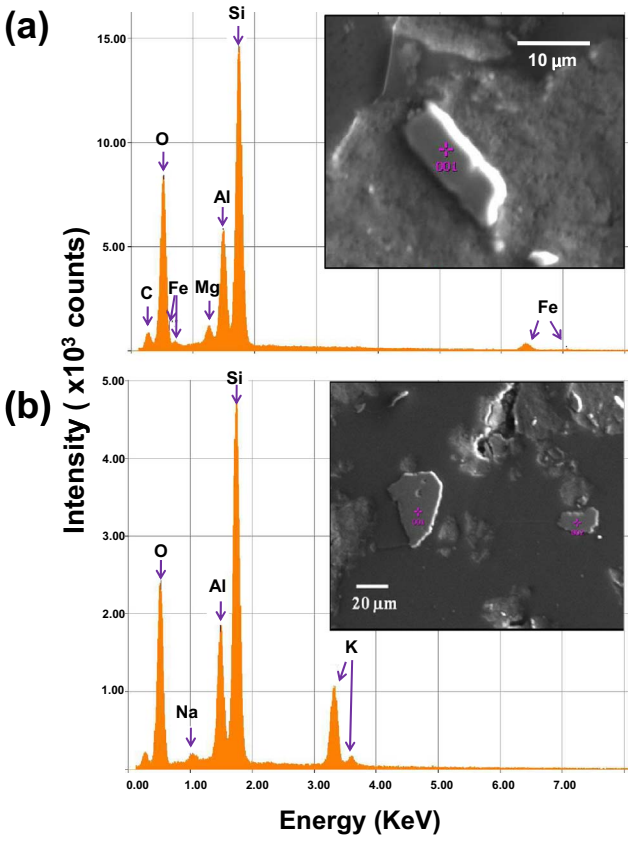

Fig. 3. a) Image of a montmorillonite particle and the corresponding EMPA. b) The same for a feldspar particle. The peak carbon is due to the carbon coating to make conductive the sample.

rhodonite (Mn), sodalite (Cl), topaz (F), chromite (Cr), baryte (Ba) and zinc oxide (Zn). Similar to the results obtained by XRD, the micropobe analysis determined that montmorillonite was the main mineral present in the sample. Other accessory minerals detected were chromite, baritine, apatite, baddeleyite, ilmenite, magnetite, monazite, quartz, plagioclase, zircon and K-feldspars. Fig. 3 (a) and Fig. 3 (b) show the image of a montmorillonite particle and a feldspar particle together with their corresponding EMPA spectra. According to the results of the EMPA analysis (seven measures), the chemical formula of the montmorillonite studied here is:

$$(Ca_{0.029}Na_{0.019}K_{0.030})(Si_{3.993}Al_{0.007})^{IV}(Al_{1.557}Ti_{0.005}Fe_{0.2053}Mg_{0.3158})^{VI}(OH)_2.$$

2.1.3. Specific surface area

The specific surface area (SSA) was measured by the single-point N_2 adsorption method with a STROHLEIN area meter II instrument, and the methylene blue adsorption method (e.g. Avena et al., 2001). For the former method, a certain amount of dried solid, previously outgassed at 105 °C, was placed in contact with N_2 and the system was cooled to 77 K to produce and quantify the gas adsorption. The SSA of the sample was calculated from the adsorbed amount, taking into account that each N_2 molecule covers an area of 16Å^2. The SSA obtained for the particles was 12 $m^2\,g^{-1}$. This value represents the external surface area of the clay mineral and was rather for montmorillonite, since nitrogen molecules cannot enter in the interlayer spacing. Conversely, the SSA obtained using the methylene blue adsorption method was higher (833 $m^2\,g^{-1}$). The difference between the data obtained following both methodologies is explained because the methylene blue adsorption method determines both the external and internal surface area.

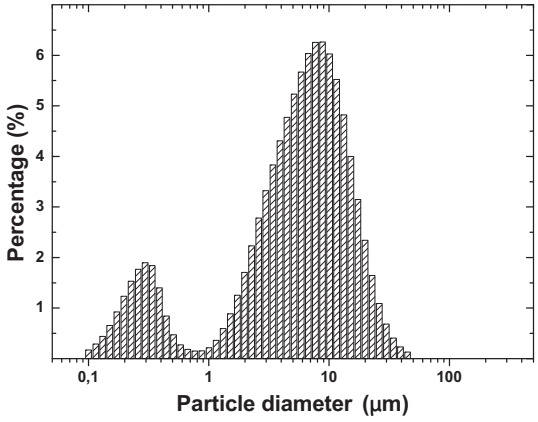

Fig. 4. Particle size distribution of the sample in milliQ water.

2.1.4. Dynamic light scattering

The grain size distribution of the sampled particles was measured by dynamic light scattering (DLS) using a Horiba LA 950 particle size analyzer. The reproducibility of data was tested using polydisperse particle standards (PS202/3–30 μm and PS215/10–100 μm, Whitehouse Scientific). Ionic strength, pH, and time of sonication are variables that can promote aggregation (Borgnino, 2013). This is why in this work the particle size was only measured in milliQ water in order to reproduce the real conditions at which particles can be immersed in water droplets. Thus, the particles did not allow to be aggregated due to changes in the external conditions, as pH and ionic strength. Three different conditions of sonication time, circulation and agitation speeds were used to determine the particle size distribution. For all these conditions the statistically same distribution was obtained. For one of these conditions, Fig. 4 shows the size distribution of the particles in the sample, which corresponds to a bimodal distribution. The smallest particles were centered at 0.3 μm, while the larger particles were between 7 and 8 μm. This bimodal distribution is typical for clay particles where aggregation occurs (Cadene et al., 2005; Poli et al., 2008).

2.2. Droplet freezing experiments

Droplets with different volumes containing different concentrations of dust particles were tested by the immersion freezing mechanism. To prepare the suspensions, a known mass of the sample was weighed by using a microbalance (Mettler-Toledo XP205, UK), which was directly suspended in a known volume of Milli-Q water (an electrical conductivity of 0.054 μS cm^{-1}). Then, this preparation was diluted and a total of six suspensions of different concentrations were prepared (2, 0.2, 0.08, 0.04 and 0.008 mg mL^{-1}). For each of these suspensions, around 40 droplets of different volumes were analyzed (2.5, 5, 10, 25, 50, 75 and 100 μL) (radius = 0.84, 1.06, 1.33, 1.81, 2.28, 2.61 and 2.88 mm, respectively). For comparison purposes, drops of pure Milli-Q water were also analyzed for all these volumes since the freezing temperature of these droplets represents the background temperature.

Droplet freezing experiments were performed to analyze the role of the collected dust particles as INPs by immersion freezing mode. The experimental device consisted of a metallic plate placed on a Peltier cooling device. The droplets were deposited on a thin Teflon ribbon covering the plate to avoid ice formation on the plate surface during the cooling process and to preserve the geometry of the drop. Every single droplet was collected in a pipette and placed on the surface of the Teflon ribbon. The temperature of the drop was lowered at a constant rate of 1 °C min^{-1} (e.g. Ardon-Dryer and Levin, 2014). A perforation in the cross section of the plate allowed fixing a calibrated thermocouple for measuring the temperature while it was gradually decreasing. This device was placed in a cold chamber settled at 0 °C. The evolution of the drop during the decrease in the temperature was followed with a USB digital microscope placed in the cold chamber. Since the microscope can detect the changes in the reflectivity and opacity of the drops after their freezing, the temperature when the drop is freezing can be detected. For each experiment, the Teflon ribbon was replaced. After the drop was placed on the Teflon ribbon, the device was put in the cold chamber at 0 °C for about 20 min in order to let the system reach the thermal equilibrium. By following this procedure, the freezing temperatures of individual droplets of different volumes and concentrations were obtained. The main advantage of this technique is the control of the droplet size and concentration. This control of the freezing temperature of individual droplets improves the experimental statistics. In general, it was observed that the droplets in contact with Teflon kept their spherical shape. The difference between theoretical diameters (estimated from the volume) and those obtained from photographs of the drops were in all cases lower than 5%. This kind of experimental setup has been widely used for immersion freezing studies (e.g. Tobo, 2016; Whale et al., 2015a, 2015b; Ardon-Dryer and Levin, 2014).

3. Results and discussion

3.1. Behavior of the freezing temperature

The effects of the particle concentration and the drop volume on the freezing temperature (T_f) were analyzed. For each droplet volume, an increase in T_f was observed with increasing suspension concentration. This is in agreement with results previously reported for other kinds of mineral aerosols (e.g. Kaufmann et al., 2016; Peckhaus et al., 2016; Pinti et al., 2012). As an example, Fig. 5 shows the box plots of T_f for droplets of 2.5 μL in volume and for the different analyzed suspension concentrations.

Although T_f increased with increasing suspension concentration, note that T_f tended to a plateau with the highest concentrations. This same behavior was observed for all the droplet volumes (not shown).

The relation between the volume and the freezing temperature for pure water has been reported by several authors for > 60 years (Heverly, 1949; Pruppacher and Klett, 1997). In order to compare the current results with those obtained from other authors, the following relation was used to fit the freezing temperature as a function of the drop volume:

$$T_{sm} = a - b \ln V \quad (1)$$

where T_{sm} is the modulus of the median freezing temperature (°C), V is the droplet volume (μL), and a and b are fitting parameters. In this work, the fitting corresponds to the values $a = 15.17 \pm 0.66$ and $b = 0.06 \pm 0.01$, with the interval of values being previously reported (Pruppacher and Klett, 1997 and references therein).

The behavior of T_f versus the droplet volume was analyzed for each suspension concentration. For example, Fig. 6 shows the box plots of the freezing temperature for 2 mg mL^{-1} as a function of the different analyzed drop volumes.

It can be seen that when the drop volume increased, T_f also increased. For droplets containing dust particles, the increase in T_f with the increase in volume can be explained because smaller droplets contain less surface area of soil. As a consequence, these droplets will have, on average, a smaller sample of active sites available to nucleate ice. Because of the small number of efficient active sites, these droplets will have a lower probability of nucleating ice and therefore they will freeze at lower temperatures. Conversely, larger droplets will contain more area of soil and a higher number of active sites, and thus they will freeze at warmer temperatures (e.g. O'Sullivan et al., 2014). For this reason, for a constant concentration, if the drop volume increases the number of active sites should be also higher. The behavior observed in Fig. 5 can be explained considering that the increase in the particle concentration can promote aggregation (Borgnino, 2013). Even though in some experiments it has been shown that the influence of the degree of agglomeration and the random placement of the particles in the drop

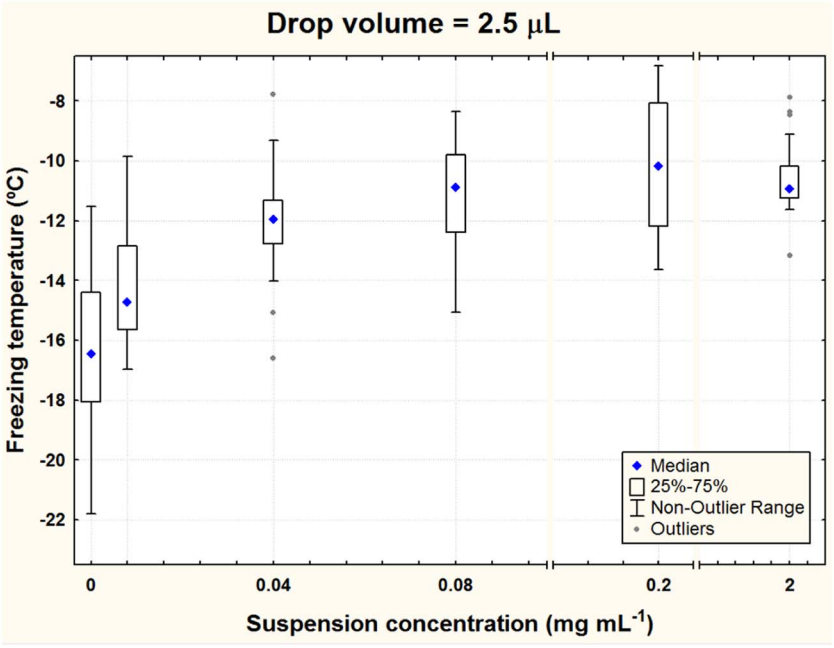

Fig. 5. Box plots of freezing temperature as a function of different suspension concentration for drops of 2.5 µL.

on the estimation of the density of active sites promoting ice nucleation seems to be small (e.g. Hiranuma et al., 2015), the effect of aggregation on the availability of active sites can explain the plateau in the T_f values at higher suspension concentrations.

3.2. Determination of the ice active surface site density

Since T_f values are dependent on droplet volume and suspension concentration, among other variables, the efficiency with which a material nucleates ice is frequently normalized to the nucleation sites per unit surface area. This normalization neglects the role of time dependence in nucleation and assumes that the ice nucleation occurs on the specific active sites of the INP when a characteristic temperature is reached (Fletcher, 1969). Then, the cumulative number of active sites per unit of droplet volume at a given temperature ($K(T)$) can be calculated through the fraction of frozen droplets at that temperature ($f_{frozen}(T)$) as:

$$K(T) = -\frac{\ln(1 - f_{frozen}(T))}{V_d} \quad (2)$$

where V_d is the volume of the droplets (Vali, 1971). By assuming that the mass of particles is distributed uniformly inside droplets with the same volume, the ice nucleation active site density per unit of mass for a given T ($n_m(T)$) can be expressed as:

$$n_m(T) = K(T) \cdot \frac{d}{C_m} \quad (3)$$

Finally, if the approximate surface area per mass is known, the number of ice nucleation active site per unit of surface area at a certain T ($n_s(T)$) can be determined as (e.g. Tobo, 2016):

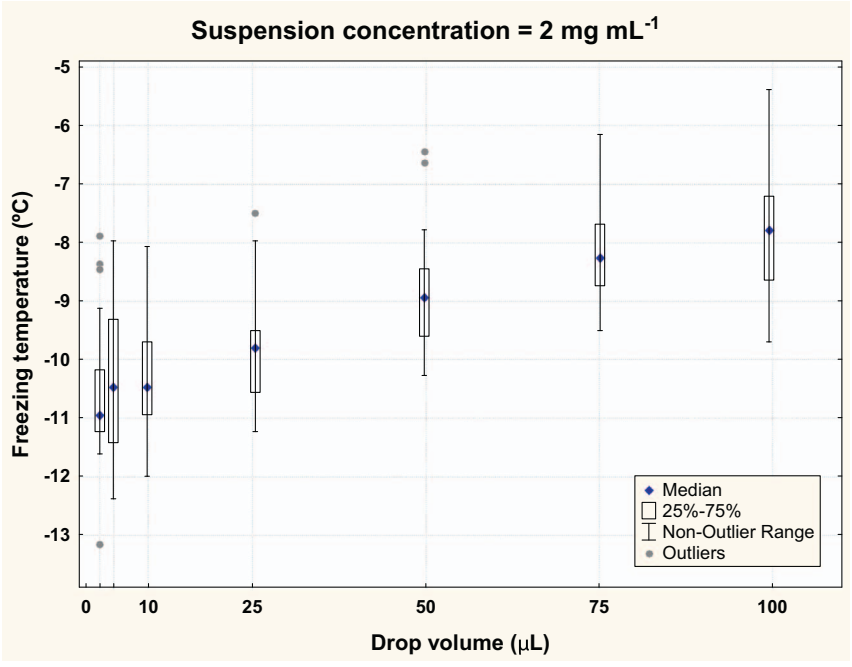

Fig. 6. Box plots of freezing temperature as a function of different drop volumes for suspension concentration of 2 mg mL^{-1}.

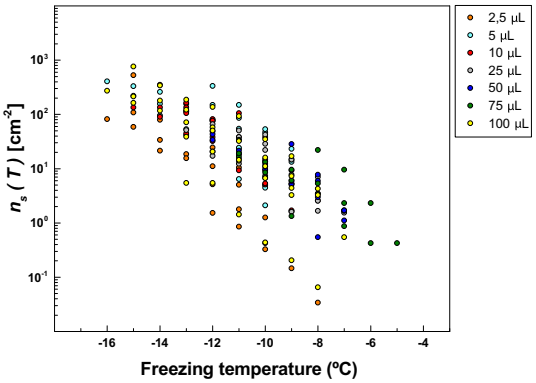

Fig. 7. Active sites per unit of surface area with temperature ($n_s(T)$) values obtained for drops in different volumes.

$$n_s(T) = n_m(T) \cdot \left(\frac{S_{total}}{M_{total}}\right)^{-1} \quad (4)$$

where S_{total}/M_{total} is the surface-to-mass ratio of the particles.

$n_s(T)$ is widely used to describe the heterogeneous nucleation efficiency. Therefore, following the previous equations $n_s(T)$ was calculated for the analyzed sample. S_{total}/M_{total} was considered equal to $12\,m^2\,g^{-1}$ from the single-point N_2 adsorption method (see section 2.1.3).

The obtained $n_s(T)$ values are shown in Fig. 7. They were compared to data and parameterizations previously reported and are shown in Fig. 8 for soil and dust samples collected at different sites, such as Canary Island (Niemand et al., 2012), Israel (Niemand et al., 2012; Reicher et al., 2018), the Takla Makan Desert, in China, and a site collected 50 km north of Cairo city, Egypt (Niemand et al., 2012 and Connolly et al., 2009). From now on, these two last samples will be referred as from Asia and Sahara, respectively. The parameterization reported by Niemand et al. (2012) for Asia is also shown. Finally, data and parameterizations reported for K-feldspars were also included in the figure, considering that this mineral compose the studied sample and also considering they have shown to be efficient ice nuclei (e.g. Atkinson et al., 2013). In this way, $n_s(T)$ values for K-feldspar reported by Niedermeier et al. (2015) and Reicher et al. (2018) are shown. Since feldspar mass content in natural soils typically varies between 1 and 25%, Atkinson et al. (2013) report a parameterization of $n_s(T)$ for pure K-feldspars but also a scaled n_s(T) values assuming the presence of K-feldspar in the surface of natural dust particles. Both, the parameterization and the scaled values, were also included in the figure.

From Fig. 7 observe that our derived $n_s(T)$ values, independently of the droplet volume, present a high dispersion. This variability and the fact that the $n_s(T)$ do not converge to a single function is a new evidence of the possible aggregation of the particles. The range of our $n_s(T)$ are in agreement to those previously reported for the analyzed range of temperature. They are contained between the fit of K-feldspars and the scaled area from Atkinson et al. (2013). In order to obtain a parameterization covering the wide range of temperatures, measurements of T_f for droplets at lower volumes would be useful to determine the $n_s(T)$ values at lower temperatures.

3.3. Particles promoting ice nucleation

In order to analyze the characteristics of the collected particles promoting ice nucleation, a comparison of the bibliography data previously reported studying the chemical properties of mineral particles acting as INPs was made. Regarding the composition of particles, montmorillonite and other clays with inherent porosity can preactivate the ice nucleation (Marcolli, 2017). It has also been suggested that alkali feldspars make mineral dust an effective INP (Atkinson et al., 2013; Kiselev et al., 2016; Harrison et al., 2016). In the same way, Augustin-Bauditz et al. (2014) found that microcline feldspar nucleates ice more efficiently than other minerals, while Kaufmann et al. (2016) highlighted the importance of determining particle acting as INP by immersion freezing has a microcline structure. Considering these results, a more detailed analysis of the XRD spectra was carried out with emphasis being placed on knowing the polymorphic form of the sampled particles. The Panalytical X'Pert High Score software was used again to obtain the diffractograms, which were interpreted using powder diffraction pattern files from the Powder Diffraction File (PDF). Table 1 shows the characteristics of the main accessory compounds that make up the sample (besides montmorillonite): the mineral name, chemical formula, crystal system and the reference code of the pattern file.

Note that alkali feldspars with microcline structures are present as accessory compounds. Then, considering the results from literature, it can be concluded that even though montmorillonite was the main mineral in the collected sample, these accessory minerals deserve to be analyzed in detail in order to know if they could be responsible for the ability of the collected particles to act as INPs.

4. Summary and concluding remarks

Results show that the natural minerals collected in Neuquén, the Patagonian area of Argentina, are effective ice nuclei particles by immersion freezing mode. The increase in the freezing temperature of the drops was variable depending on the volume of these drops and the suspension concentration. A parameterization of the increase in the

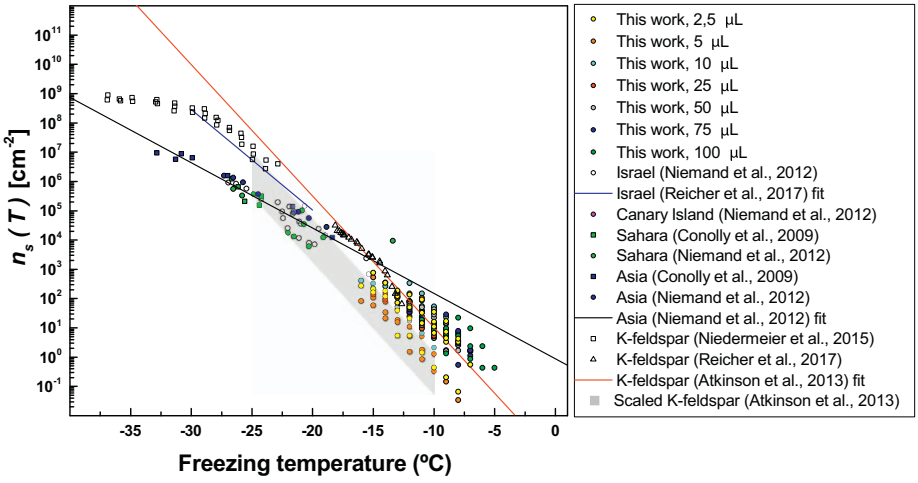

Fig. 8. Active sites per unit of surface area with temperature ($n_s(T)$) values reported in the present work and those determined in other studies for different kind of particles.

Table 1
Characteristics of the main accessories minerals of the collected sample, obtained by comparison from powder diffraction patterns.

Compound name	Mineral name	Chemical formula	Crystal system	Reference code
Silicon oxide	Quartz	SiO_2	Hexagonal	01-089-8934
K-Al silicate hydroxide	Muscovite	$KAl_2Si_3AlO_{10}(OH)_2$	Monoclinic	00-007-0025
K-Al silicate	Orthoclase	$KAlSi_3O_8$	Monoclinic	00-019-0931
Na-Ca-Al silicate	Anorthite	$(Ca,Na)\ (Si,Al)_4O_8$	Anorthic	00-018-1202

freezing temperature with the suspension concentration is shown for different drop volumes. The plateau in the freezing temperature observed for the highest suspension concentrations was related to the aggregation of the particles when the concentration was increased. This aggregation would lead to the loss of the active sites promoting ice nucleation. For a given suspension concentration, an increase in the freezing temperature of the drops was observed when the drop volumes were increased. This behavior can be explained considering that, for a constant suspension concentration, the number of dust particles contained in each drop is larger when the drop volume increases. Consequently, the number of active sites increases with the drop volume. Thus, the ice nucleation probability at warmer temperatures will be enhanced for larger drop volumes. For the studied range of temperature, the number of active sites per unit of surface area was calculated and was in agreement with those reported for different sites and particles. The dispersion in the reported values would confirm the aggregation of the particles. The ability of the collected particles to act as INPs by immersion freezing was analyzed considering the components in the sample. From the analysis of the XRD spectra and the EMPA measurements, it was found that the main component in the sample was montmorillonite. However, even though previous studies assumed that clay minerals are responsible for the ability of natural dust particles to act as INPs, more recent studies show that feldspars can be responsible for this ability. By comparing the XRD spectra with powder diffraction patterns, it was found that the accessory minerals composing the particles were quartz, muscovite, orthoclase, and anorthite. Considering that from literature the alkali feldspars and, at the same time, the microcline feldspars were related to the ability of the particles as INPs, these accessory minerals deserve to be studied in detail. This is the first work studying the role of Patagonian minerals as INPs. These results are relevant considering that Patagonia is one of the most important arid regions and source of natural mineral particles in the atmosphere.

Acknowledgements

We thank Secretaría de Ciencia y Tecnología de la Universidad Nacional de Córdoba (UNC) (2016-2017), Consejo Nacional de Investigaciones Científicas y Tecnológicas (CONICET) (PIP 2013-2015), and Agencia Nacional de Promoción Científica (FONCYT) (PICT 2013-1713; PICT 2015-2644) for the support.

References

Ardon-Dryer, K., Levin, Z., 2014. Ground-based measurements of immersion freezing in the eastern Mediterranean. Atmos. Chem. Phys. 14, 5217–5231.
Atkinson, J.D., Murray, B.J., Woodhouse, M.T., Whale, T.F., Baustian, K.J., Carslaw, K.S., Dobbie, S., O'Sullivan, D., Malkin, T.L., 2013. The importance of feldspar for ice nucleation by mineral dust in mixed-phase clouds. Nature 498 (7454), 355–358.
Augustin-Bauditz, S., Wex, H., Kanter, S., Ebert, M., Stolz, F., Prager, A., Niedermeier, D., Stratmann, F., 2014. The immersion mode ice nucleation behavior of mineral dusts: a comparison of different pure and surface modified dusts. Geophys. Res. Lett. 41, 7375–7382.
Avena, M.J., Valenti, L., Pfaffen, V., De Pauli, C.P., 2001. Methylene blue dimerization does not interference in surface-area measurements of kaolinite and soils. Clays Clay Min. 49, 168–173.
Belosi, F., Santachiara, G., Prodi, F., 2014. Ice-forming nuclei in Antarctica: new and past measurements. Atmos. Res. 145-146, 105–111.
Belosi, F., Rinaldi, M., Decesari, S., Tarozzi, L., Nicosia, A., Santachiara, G., 2017. Ground level ice nuclei particle measurements including Saharan dust events at a Po Valley rural site (san Pietro Capofiume, Italy). Atmos. Res. 186, 116–126.
Boose, Y., Welti, A., Atkinson, J., Ramelli, F., Danielczok, A., Bingemer, H.G., Plötze, M., Sierau, B., Kanji, Z.A., Lohmann, U., 2016. Heterogeneous ice nucleation on dust particles sourced from nine deserts worldwide - part 1: immersion freezing. Atmos. Chem. Phys. 16, 15075–15095.
Borgnino, L., 2013. Experimental determination of the colloidal stability of Fe(III)-montmorillonite: effects of organic matter, ionic strength and pH conditions. Colloids and Surfaces A: Physicochem. Eng. Aspects 423, 178–187.
Borgnino, L., Avena, M., De Pauli, P., 2009. Synthesis and characterization of Fe(III)-montmorillonites for phosphate adsorption. Colloids Surf. A: Physicochem. Eng. Aspects 341, 46–52.
Cadene, A., Durand-Vidal, S., Turq, P., Brendle, J., 2005. Study of individual Na-montmorillonite particles size, morphology, and apparent charge. J. Colloid Interface Sci. 285, 719–730.
Connolly, P.J., Möhler, O., Field, P.R., Saathoff, H., Burgess, R., Choularton, T., Gallagher, M., 2009. Studies of heterogeneous freezing by three different desert dust samples. Atmos. Chem. Phys. 9, 2805–2824. http://dx.doi.org/10.5194/acp-9-2805-2009.
Domínguez, E.A., Mas, G.R., Cravero, F., 2001. A clay odyssey. In: Proceedings of the 12th International Clay Conference, Bahía Blanca, Argentina, July 22–28, 2001. Elsevier, pp. 505–512.
Fletcher, N.H., 1969. Active sites and ice crystal nucleation. J. Atmos. Sci. 26, 1266–1271.
Formenti, P., Schütz, L., Balkanski, Y., Desboeufs, K., Ebert, M., Kandler, K., Petzold, A., Scheuvens, D., Weinbruch, S., Zhang, D., 2011. Recent progress in understanding physical and chemical properties of African and Asian mineral dust. Atmos. Chem. Phys. 11, 8231–8256.
Formenti, P., Caquineau, S., Desboeufs, K., Klaver, A., Chevaillier, S., Journet, E., Rajot, J.L., 2014. Mapping the physico-chemical properties of mineral dust in western Africa: mineralogical composition. Atmos. Chem. Phys. 14, 10663–10686.
Fröhlich-Nowoisky, J., Kampf, C.J., Weber, B., Huffman, J.A., Pöhlker, C., Andreae, M.O., Lang-Yona, N., Burrows, S.M., Gunthe, S.S., Elbert, W., Su, H., Hoor, P., Thines, E., Hoffmann, T., Després, V.R., Pöschl, U., 2016. Bioaerosols in the earth system: climate, health, and ecosystem interactions. Atmos. Res. 182, 346–376.
Gaiero, D.M., Probst, J.-L., Depetris, P.J., Bidart, S.M., Leleyter, L., 2003. Iron and other transition metals in Patagonian riverborne and windborne materials: geochemical control and transport to the southern South Atlantic Ocean. Geochim. Cosmochim. Acta 67, 3603–3623.
Gaiero, D.M., Depetris, P.J., Probst, J.L., Bidart, S.M., Leleyter, L., 2004. The signature of river- and wind-borne materials exported from Patagonia to the southern latitudes: a view from REEs and implications for paleoclimatic interpretations. Earth Planet. Sci. Lett. 219, 357–376.
Gassó, S., Stein, A., Marino, F., Castellano, E., Udisti, R., Ceratto, J., 2010. A combined observational and modeling approach to study modern dust transport from the Patagonia desert to East Antarctica. Atmos. Chem. Phys. 10, 8287–8303.
Ginoux, P., Prospero, J.M., Gill, T.E., Hsu, N.C., Zhao, M., 2012. Global-scale attribution of anthropogenic and natural dust sources and their emission rates based on MODIS deep blue aerosol products. Rev. Geophys. 50, RG3005.
Harrison, A.D., Whale, T.F., Carpenter, M.A., Holden, M.A., Neve, L., O'Sullivan, D., Vergara Temprado, J., Murray, B.J., 2016. Not all feldspars are equal: a survey of ice nucleating properties across the feldspar group of minerals. Atmos. Chem. Phys. 16, 10927–10940.
Hazra, A., Padmakumari, B., Maheskumar, R.S., Chen, J.P., 2016. The effect of mineral dust and soot aerosols on ice microphysics near the foothills of the Himalayas: a numerical investigation. Atmos. Res. 171, 41–55.
Heverly, J.R., 1949. Supercooling and crystallization. Earth & Space Science News 30, 205–210.
Hiranuma, N., Augustin-Bauditz, S., Bingemer, H., Budke, C., Curtius, J., Danielczok, A., Diehl, K., Dreischmeier, K., Ebert, M., Frank, F., Hoffmann, N., Kandler, K., Kiselev, A., Koop, T., Leisner, T., Möhler, O., Nillius, B., Peckhaus, A., Rose, D., Weinbruch, S., Wex, H., Boose, Y., DeMott, P.J., Hader, J.D., Hill, T.C.J., Kanji, Z.A., Kulkarni, G., Levin, E.J.T., McCluskey, C.S., Murakami, M., Murray, B.J., Niedermeier, D., Petters, M.D., O'Sullivan, D., Saito, A., Schill, G.P., Tajiri, T., Tolbert, M.A., Welti, A., Whale, T.F., Wright, T.P., Yamashita, K., 2015. A comprehensive laboratory study on the immersion freezing behavior of illite NX particles: a comparison of 17 ice nucleation measurement techniques. Atmos. Chem. Phys. 15, 2489–2518.
Hoose, C., Möhler, O., 2012. Heterogeneous ice nucleation on atmospheric aerosols: a review of results from laboratory experiments. Atmos. Chem. Phys. 12, 9817–9854.
Hoose, C., Kristjánsson, J.E., Chen, J.-P., Hazra, A., 2010. A classical-theory-based parameterization of heterogeneous ice nucleation by mineral dust, soot, and biological particles in a global climate model. J. Atmos. Sci. 67, 2483–2503.
Impiccini, A., Vallés, J.M., 2002. Los depósitos de bentonita de Barda Negra y cerro Bandera, departamento Zapala, provincia del Neuquén, Argentina. Rev. Asoc. Geol. Argent. 57 (3), 305–314.
Isono, K., Komabayasi, M., Ono, A., 1959. The nature and origin of ice nuclei in the atmosphere. J. Meteor. Soc. Japan 37, 211–233.
Johnson, M.S., Meskhidze, N., Solmon, F., Gassó, S., Chuang, P.Y., Gaiero, D.M.,

Yantosca, M., Wu, S., Wang, Y., Carouge, C., 2010. Modeling dust and soluble iron deposition to the South Atlantic Ocean. J. Geophys. Res. 115, D15202.
Kaufmann, L., Marcolli, C., Hofer, J., Pinti, V., Hoyle, C.R., Peter, T., 2016. Ice nucleation efficiency of natural dust samples in the immersion mode. Atmos. Chem. Phys. 16, 1177–11206.
Kiselev, A., Bachmann, F., Pedevilla, P., Cox, S.J., Michaelides, A., Gerthsen, D., Leisner, T., 2016. Active sites in heterogeneous ice nucleation – the example of K-rich feldspars. Science 355, 367–371.
Marcolli, C., 2017. Pre-activation of aerosol particles by ice preserved in pores. Atmos. Chem. Phys. 17, 1595–1622.
McCartney, G.C., 1934. The bentonites and closely related rocks of Patagonia. Am. Mus. Novit. 630, 1–16.
Murray, B.J., O'Sullivan, D., Atkinson, J.D., Webb, M.E., 2012. Ice nucleation by particles immersed in supercooled cloud droplets. Chem. 30 Soc. Rev. 41, 6519–6554.
Nagare, B., Marcolli, C., Welti, A., Stetzer, O., Lohmann, U., 2016. Comparing contact and immersion freezing from continuous flow diffusion chambers. Atmos. Chem. Phys. 16, 8899–8914.
Niedermeier, D., Augustin-Bauditz, S., Hartmann, S., Wex, H., Ignatius, K., Stratmann, F., 2015. Can we define an asymptotic value for the ice active surface site density for heterogeneous ice nucleation? J. Geophys. Res. Atmos. 120, 5036–5046.
Niemand, M., Möhler, O., Vogel, B., Vogel, H., Hoose, C., Connolly, P., Klein, H., Bingemer, H., DeMott, P., Skrotzki, J., Leisner, T., 2012. A particle-surface-area-based parameterization of immersion freezing on desert dust particles. J. Atmos. Sci. 69, 3077–3092. http://dx.doi.org/10.1175/jas-d-11-0249.1.
O'Sullivan, D., Murray, B.J., Malkin, T.L., Whale, T.F., Umo, N.S., Atkinson, J.D., Price, H.C., Baustian, K.J., Browse, J., Webb, M.E., 2014. Ice nucleation by fertile soil dusts: relative importance of mineral and biogenic components. Atmos. Chem. Phys. 14, 1853–1867.
Peckhaus, A., Kiselev, A., Hiron, T., Ebert, M., Leisner, T., 2016. A comparative study of K-rich and Na/Ca-rich feldspar ice-nucleating particles in a nanoliter droplet freezing assay. Atmos. Chem. Phys. 16, 11477–11496.
Pinti, V., Marcolli, C., Zobrist, B., Hoyle, C.R., Peter, T., 2012. Ice nucleation efficiency of clay minerals in the immersion mode. Atmos. Chem. Phys. 12, 5859–5878.
Poli, A.L., Batista, T., Schmitt, C.C., Gessner, F., Neumann, M.G., 2008. Effect of sonication on the particle size of montmorillonite clays. J. Colloid Interface Sci. 325, 386–390.
Popovicheva, O., Kireeva, E., Persiantseva, N., Khokhlova, T., Shonija, N., Tishkova, V., Demirdjian, B., 2008. Effect of soot on immersion freezing of water and possible atmospheric implications. Atmos. Res. 90, 326–337.
Prospero, J.M., Ginoux, P., Torres, O., Nicholson, S.E., Gill, T.E., 2002. Environmental characterization of global sources of atmospheric soil dust identified with the nimbus 7 total ozone mapping spectrometer (TOMS) absorbing aerosol product. Rev. Geophys. 40, 1002.
Pruppacher, H.R., Klett, J.D., 1997. Microphysics of Clouds and Precipitation, Atmospheric and Oceanographic Sciences Library. Kluwer Academic Publishers, Dordrecht, The Netherlands.
Ramsperger, B., Herrmann, L., Stahr, K., 1998a. Dust characteristics and source-sink relations in eastern West Africa (SWNiger and Benin) and South America (Argentinian Pampas). Z. Pflanzenernahr. Bodenk. 161, 357–363.
Ramsperger, B., Peinemann, N., Stahr, K., 1998b. Deposition rates and characteristics of aeolian dust in the semi-arid and sub-humid regions of 10 the Argentinian Pampa. J. Arid Environ. 39, 467–476.
Reicher, N., Segev, L., Rudich, Y., 2018. The WeIzmann Supercooled droplets observation (WISDOM) on a microarray and application for ambient dust. Atmos. Meas. Tech. Discuss. 11, 233–248.
Santachiara, G., Di Matteo, L., Prodi, F., Belosi, F., 2010. Atmospheric particles acting as ice forming nuclei in different size ranges. Atmos. Res. 96, 266–272.
Satheesh, S.K., Moorthy, K.K., 2005. Radiative effects of natural aerosols: a review. Atmos. Environ. 39, 2089–2110.
Tegen, I., Fung, I., 1994. Modeling of mineral dust in the atmosphere: sources, transport, and optical thickness. J. Geophys. Res. 99, 22897–22914.
Tobo, Y., 2016. An improved approach for measuring immersion freezing in large droplets over a wide temperature range. Sci. Rep. 6, 32930.
Vali, G., 1971. Quantitative evaluation of experimental results on the heterogeneous freezing nucleation of supercooled liquids. J. Atmos. Sci. 28, 402–409.
Vali, G., 1985. Nucleation terminology, J. Aerosol S. 16 (6), 575–576.
Von Blohn, N., Mitra, S.K., Diehl, K., Borrmann, S., 2005. The ice nucleating ability of pollen part III: new laboratory studies in immersion and contact freezing modes including more pollen types. Atmos. Res. 78, 182–189.
Wex, H., DeMott, P.J., Tobo, Y., Hartmann, S., Rösch, M., Clauss, T., Tomsche, L., Niedermeier, D., Stratmann, F., 2014. Kaolinite particles as ice nuclei: learning from the use of different kaolinite samples and different coatings. Atmos. Chem. Phys. 14, 5529–5546.
Whale, T.F., Murray, B.J., O'Sullivan, D., Wilson, T.W., Umo, N.S., Baustian, K.J., Atkinson, J.D., Workneh, D.A., Morris, G.J., 2015a. A technique for quantifying heterogeneous ice nucleation in microlitre supercooled water droplets. Atmos. Meas. Tech. 8, 2437–2447.
Whale, T.F., Murray, B.J., O'Sullivan, D., Wilson, T.W., Umo, N.S., Baustian, K.J., Atkinson, J.D., Workneh, D.A., Morris, G.J., 2015b. A technique for quantifying heterogeneous ice nucleation in microlitre supercooled water droplets. Atmos. Meas. Tech. 8, 2437–2447.
Yang, J., Lei, H., Hu, Z., Hou, T., 2014. Particle size spectra and possible mechanisms of high ice concentration in nimbostratus over Hebei Province, China. Atmos. Res. 142, 79–90.